Accepted Manuscript

Inhibitor of the human telomerase reverse trancriptase (hTERT) gene promoter induces cell apoptosis via a mitochondrial-dependent pathway

Yuyin Li, Guojun Pan, Yue Chen, Qian Yang, Tiantian Hao, Lianbo Zhao, Long Zhao, Yusheng Cong, Aipo Diao, Peng Yu

PII: S0223-5234(17)31108-X

DOI: 10.1016/j.ejmech.2017.12.077

Reference: EJMECH 10055

To appear in: *European Journal of Medicinal Chemistry*

Received Date: 27 June 2017

Revised Date: 20 December 2017

Accepted Date: 22 December 2017

Please cite this article as: Y. Li, G. Pan, Y. Chen, Q. Yang, T. Hao, L. Zhao, L. Zhao, Y. Cong, A. Diao, P. Yu, Inhibitor of the human telomerase reverse trancriptase (hTERT) gene promoter induces cell apoptosis via a mitochondrial-dependent pathway, *European Journal of Medicinal Chemistry* (2018), doi: 10.1016/j.ejmech.2017.12.077.

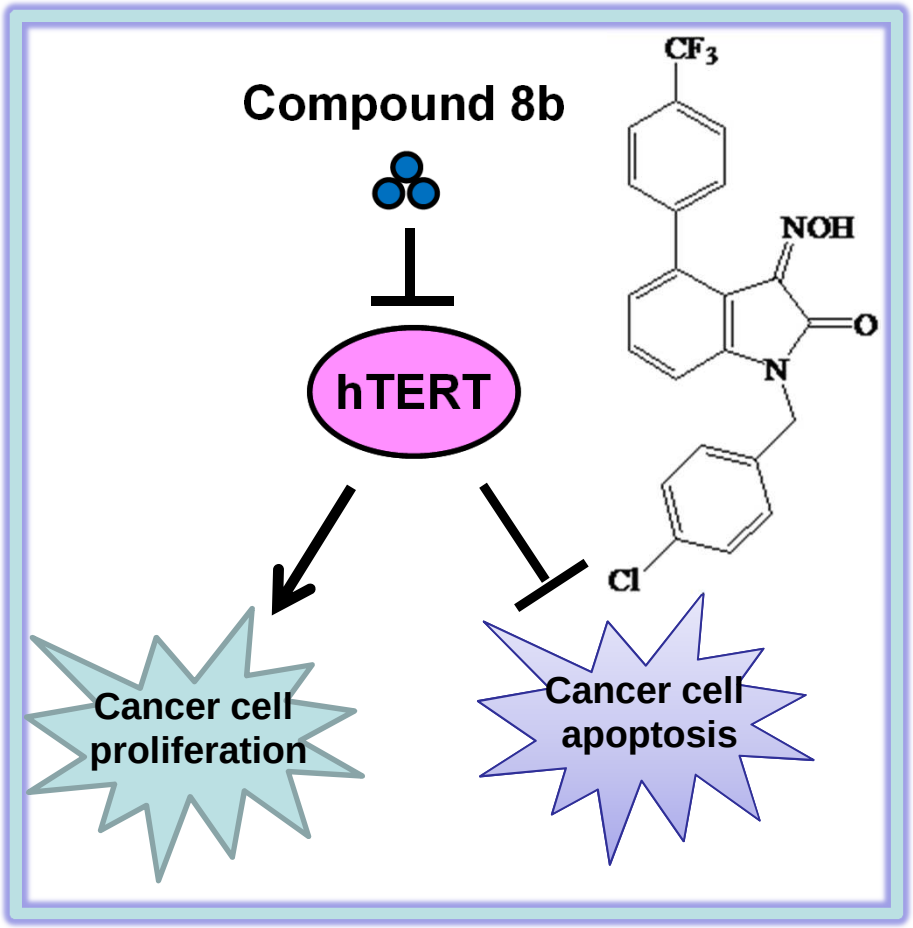
Compound 8b
hTERT
CF3
NOH
O
N
Cl
Cancer cell proliferation
Cancer cell apoptosis

Inhibitor of the human telomerase reverse trancriptase (hTERT) gene promoter induces cell apoptosis via a mitochondrial-dependent pathway

Yuyin Li[a, 1], Guojun Pan[b, 1], Yue Chen[a], Qian Yang[a], Tiantian Hao[b], Lianbo Zhao[b], Long Zhao[b], Yusheng Cong[c], Aipo Diao[a, *], Peng Yu[b, *]

[a] *School of Biotechnology, Tianjin University of Science and Technology, Key Lab of Industrial Fermentation Microbiology of the Ministry of Education, Tianjin, 300457, China.*
[b] *China International Science and Technology Cooperation Base of Food Nutrition/Safety and Medicinal Chemistry, Sino-French Joint Lab of Food Nutrition/Safety and Medicinal Chemistry, Tianjin University of Science and Technology, Tianjin 300457, China.*
[c] *Institute of Aging Research, Hangzhou Normal University, School of Medicine, Hangzhou, Zhejiang Province 311121, China*

[1] These authors contributed equally to this work.
* Corresponding author.
E-mail addresses: diaoaipo@tust.edu.cn (A. Diao), yupeng@tust.edu.cn (P. Yu)

Abstract:

Telomerase is aberrantly expressed in many cancers and plays an important role in the development of cellular immortality and oncogenesis, which makes it a potential cancer therapeutic target for drug discovery. Here, we constructed a firefly luciferase reporter driven by the human telomerase reverse trancriptase (*hTERT*) gene promoter to screen for inhibitory compounds. Compound **5c** was discovered and shown to significantly inhibit the promoter activity of *hTERT* gene. Furthermore, five analogs of compound **5c** were synthesized, and compound **8b** was shown to be a more potent inhibitor of *hTERT* gene promoter activity and

subsequent expression of hTERT mRNA and protein. The viability of HeLa cells was inhibited by a knockdown of *hTERT* gene expression, and the same effect was also observed by treating with compound **8b**. Moreover, our results indicated that compound **8b** induced apoptosis of HeLa cells, and activated caspase-9 and caspase-3 enzymes. Taken together, these results suggested that compound **8b** down-regulates the expression of hTERT and induces mitochondrial-dependent apoptosis.

Keywords: hTERT; Inhibitor; Apoptosis; Synthesis

1. Introduction

Telomeres are specialized DNA structures located at the end of chromosomes, and are essential for their stabilization by protecting them from end-to-end fusion and DNA degradation[1]. In human cells, telomeres are composed of (TTAGGG)n tandem repeats. Telomerase is a unique ribonucleoprotein enzyme which is responsible for adding the telomeric repeats onto the 3’ ends of chromosome[2], Telomerase contains an internal RNA component [telomerase RNA (TR), or telomerase RNA component] and a catalytic protein with telomere-specific reverse transcriptase activity [telomerase reverse trancriptase (TERT)]. TERT which synthesises de novo telomere sequences by using TR as a template, is the rate-limiting component of the telomerase complex, and its expression is correlated with telomerase

activity [3]. Previous studies have shown that hTERT plays an important role in the development of cellular immortality and oncogenesis[4-5]. It has been shown that telomerase is aberrantly expressed in 85-90% of all human tumors, but not in their adjacent normal cells [6-9], and it plays an important role in the development of cellular immortality and oncogenesis[4, 10]. This makes telomerase a potential drug screening target for cancer therapy [11-13].

A number of studies have shown that targeting telomerase is a novel approach to targeted cancer therapeutics [14-18]. There are many potential ways to interfere with normal telomerase function, and each approach has its own strengths and weaknesses. These strategies of telomerase targeting in cancer treatment can be divided into two categories. One is targeting telomerase directly by inhibiting the activity of its catalytic subunit (hTERT) or its RNA template (hTER), leading to inhibition of telomerase activity (TA), telomere shortening and inhibition of cell proliferation. Recently, a novel dihydropyrazole-chromen controlling hTERT was designed, and it occupied high antiproliferative activity against MGC-803 cells [19]. Another strategy is by targeting the telomerase subunit indirectly with G-quadruplex stabilizers, Tankyrase or HSP90 inhibitors, thus blocking telomerase access to telomeres or inhibiting binding of telomerase-associated proteins leading to telomere uncapping and cell apoptosis. Treatment of tumor cells lines with various

telomerase inhibitors *in vitro* and *in vivo* has shown not only inhibition of TA or tumor cell proliferation, but also inhibition of tumor metastasis, indicating their potential for treatment of metastatic cancers. For example, phase I and II clinical trials with the telomerase inhibitor GRN163L were successful in determining maximum tolerated doses (MTDs) and dose-limiting toxicities (DLTs) in patients with chronic liver disease (CLD), solid tumor malignancies and breast cancer. No major cytotoxicity was observed and the inhibitor has now progressed into phase III clinical trials.

Here, we have established a firefly luciferase reporter screening system driven by *hTERT* gene promoter to screen potential compounds inhibiting hTERT expression. We identified compound **8b** that effectively inhibited the expression of hTERT by screening an initial 400 compound library. Further studies showed that compound **8b** inhibited the cell viability of HeLa cells and induced cell apoptosis via a mitochondrial-dependent pathway. These results demonstrated that compound **8b** is a potential antitumor drug for tumors expressing high levels of hTERT.

2. Results and Discussion

2.1 Chemistry

As shown in Scheme 1, The key intermediates **4a**-**4c** were readily synthesized in three steps in 55-80% yields according to the known literature procedures [20-21] which were converted into the 3-Oxime target

compounds **5a**-**5c** with NH_2OH in the presence of Pyridine. 3-NOH methylation of **5b** afforded the desired **6b** by using CH_3I in basic condition. Suzuki coupling reaction was employed to convert 4-bromo isatin **4b** into 4-(4-(trifluoromethyl)phenyl) isatin **7b** and 4-(4-methoxyphenyl) isatin **7a** respectively (Scheme 2). Compound **8a**, **8b** were prepared from **7a** and **7b** through an appropriate carbonyl group derivatization reaction.

(Scheme 1)

(Scheme 2)

2.2. Biological Evaluation

Over 400 compounds were screened for their *hTERT* expression inhibition using a firefly luciferase reporter screening system. Among them, compound 282 (**5c**, see structure in Table. 1) was found to have significant inhibitory effects on the *hTERT* gene promoter activity in a dose-dependent manner (Fig. 1A and 1B).

(Fig.1)

In order to explore the structure-activity relationship of this type of molecule against *hTERT*, a series of isatin derivatives (**5a**-**5c**, **6b**, **8a** and **8b**) were synthesized and tested for their inhibitory effects on the *hTERT* gene promoter activity in HeLa cells at concentrations of 1, 2, 4, 8, 16 μM, respectively.

As shown in table 1, compounds **5a**-**5c** which possess either chloro,

bromo or iodo groups on the C-4 position exhibited good inhibitory effects. Compound **5b** in particular has a potent EC_{50} value of 6 μM. As can be seen in table 1, conversion of 5b into 3-methyoxyimino substituted isatin destroyed the inhibitory activity, which indicated that the 3-oxime group is essential for the *hTERT* inhibition.

Inspection of the activity data of the compounds bearing chloro, bromo, methoxyphenyl and trifluoromethylphenyl groups at position C-4 suggested that a certain size of substitution at this orientation could improve the inhibition. Moreover, **8b** (4-trifluoromethylphenyl) was more potent than **8a** (4-methoxyphenyl).

(Table 1)

Since compound **8b** could inhibit the *hTERT* gene promoter activity, we next investigated whether it could down-regulate hTERT expression in HeLa cells expressing high levels of endogenous hTERT. The RT-PCR and Western blot assay results showed that compound **8b** down-regulated hTERT mRNA and protein levels (Fig. 2A-D). A dose curve (1, 2, 4, 8, 16 μM) and time course (12, 24, 36, 48 h) of hTERT expression inhibition showed that compound **8b** could down-regulate hTERT expression in a time- and dose-dependent manner (Fig. 2C-F). Furthermore, we also treated HeLa cells with compound **8b** or DMSO control for 22 generations, and measured the relative length of telomeres using Q-PCR [22-23]. As shown in Fig. 2G, compound **8b** accelerated the shortening of

telomeres. These results suggest that compound **8b** is an efficient and novel inhibitor of hTERT expression in cancer cells.

(Fig.2)

To investigate whether a knockdown of hTERT expression inhibits cell viability, RNA interference was used to reduce hTERT expression in HeLa cells. The hTERT-shRNAs were individually co-transfected with lentiviral packaging plasmids into HEK293T cells, the virus-containing supernatant was harvested and used to infect HeLa cells. Knockdown efficiency of hTERT protein was analyzed by Western blot and results showed that hTERT expression was significantly reduced after infection with hTERT-shRNAs virus-containing supernatant (Fig. 3A). To analyze the effects of endogenous hTERT knockdown on cell proliferation, MTT and colony formation assays were performed. MTT assays showed that hTERT-shRNAs transiently infected cell populations grew more slowly compared to negative control shRNA cells (Fig. 3B). Colony formation assays also showed that cells stably expressing hTERT-shRNA formed fewer colonies compared to the control (Fig. 3C and 3D). These results indicate that hTERT plays an important role in the process of cancer cell proliferation and colony formation, and that depletion of hTERT in HeLa cells inhibits cell proliferation.

(Fig.3)

Compound **8b** has been proven to be a potential inhibitor of hTERT

expression (Fig 2), and knockdown of hTERT expression in HeLa cells could inhibit cell viability (Fig 3). Thus we investigated whether compound **8b** has anti-cancer activity due to its ability for down-regulating hTERT expression. HeLa cells that have high level expression of endogenous hTERT, and L02 cells which have a lower hTERT expression were treated with an increasing dose (1, 2, 4, 8 and 16 μM) of compound **8b** for 48 h followed by MTT assay. The results suggested that compound **8b** dramatically inhibited the viability of HeLa (Fig 4A). However, the L02 cells were not sensitive to compound **8b** (Fig 4A). The compound **8b** inhibited the viability of HeLa cells in a time-dependent manner (Fig. 4B). Colony formation assays further showed that cells treated with compound **8b** formed fewer colonies compared to the control (Fig. 4C and 4D). These results indicate that compound **8b** inhibits cancer cell proliferation through the down-regulation of hTERT expression.

(Fig.4)

To elucidate the mechanism by which compound **8b** decreased cell proliferation in cancer cells containing high levels of hTERT, we investigated the effects of compound **8b** on cell apoptosis in HeLa cells. Following treatment with compound **8b** (5 μM) for 24 h, the cells were stained with DAPI. As shown in Fig 5A, HeLa cells treated with compound **8b** exhibited chromatin condensation and cell shrinkage,

which indicated a cell apoptosis phenotype. The control cells in contrast showed round and homogeneous nuclei and a regular plasma membrane shape. Similar results were also found using annexin V/PI staining with 24.5% apoptosis detected in the control cells and 59.7% apoptosis in compound **8b** treated HeLa cells, (Fig. 5B).

Apoptosis is triggered by two types of apoptotic caspases, namely initiator caspases (e.g., caspase-2, -8, -9, and -10) and effector caspases (e.g., caspase-3, -6, and -7) [24-25]. Initiator caspases cleave and activate inactive proforms of effector caspases, and activated effector caspases cleave other protein substrates to trigger the apoptotic process [26-27]. To further assess compound **8b** induced apoptotic pathway in HeLa cells, we investigated the activity level of these effector caspases. The western blotting results suggested that the level of cleaved caspase-3 increased when cells were treated with compound **8b** (Fig. 5c). Furthermore, the results also showed that compound **8b** obviously increased the cleaved caspase-9 level (activity of initiator caspases) (Fig. 5c). Considering the role of Bcl-2 family proteins in mitochondrion-dependent apoptosis, we examined the effect of compound **8b** on the expression of anti-apoptosis protein Bcl-2 and pro-apoptosis protein Bax. As shown in Fig. 5c, Bcl-2 levels were markedly decreased and Bax levels were increased in HeLa cells when cells were treated with compound **8b**. These data suggest that compound **8b** can induce apoptosis in HeLa cells via a

mitochondrial-dependent pathway.

(Fig.5)

The Bcl-2 family plays an important role in the regulation of the intrinsic, mitochondrial apoptosis. Some Bcl-2 family members protect the cell against death signals (eg. Bcl-2, Mcl-1 and Bcl-xL), while others, such as Bax, Bak, lead to caspase-9 activation and mitochondrial apoptosis. Previous studies suggest that telomerase activity plays a role in cellular resistance to apoptosis [28] and that hTERT knockdown suppresses the growth of cancer cells by inhibiting Bcl-2 [29-30]. Consistent with these studies, our results suggest that compound **8b**, which inhibits the expression of hTERT, induces cell apoptosis via a mitochondrial-dependent pathway.

3. Conclusions

In conclusion, our results indicate that compound **8b** is a novel and efficient inhibitor of hTERT expression, and that inhibition of hTERT expression could induce mitochondrial apoptosis. These results demonstrate that compound **8b** might be a promising anti-cancer drug for hTERT high-expressing tumors. Further studies should help to uncover the in-depth mechanisms for inhibition of compound **8b**. This will drive the synthesis of other analogs to more effectively inhibit hTERT expression.

4. Experimental section

4.1. Chemistry

All commercial materials and reagents were used without further purification, unless otherwise stated. Solvents were distilled prior to use. Reactions were carried out in oven-dried glassware under an inert atmosphere (nitrogen or argon). For chromatography, 200-300 mesh silica gel (Qingdao, China) was employed. ^{1}H and ^{13}CNMR spectra were recorded at 400 MHz and 100 MHz with a Brucker ARX 400 spectrometer. The chemical shifts (δ) for ^{1}H NMR spectra were given in parts per million (ppm) referenced to the residual proton signal of the duterated solvent ($CDCl_3$ at δ = 7.26 ppm, DMSO-d_6 at δ = 2.50 ppm); coupling constants were expressed in hertz δ = 77.0 ppm), DMSO-d_6 (δ = 40.0 ppm). The following abbreviations were used to describe NMR signals: s = singlet, d = doublet, t = triplet, m = multiple, and dd = doublet of doublets. HRMS were recorded on Bruker Daltonics, Inc. APEXIII 7.0 TESLA FTMS (ESI). Known products were characterized by comparison to their corresponding ^{1}H-NMR reported in the literatures.

4.2 General procedure

In a general procedure, a mixture of 4-chloroindoline-2,3-dione (4.4 mmol), K_2CO_3 (1.8 g), P-chlorobenzyl bromide (1.1 g) in DMF (10 mL) was stirred at room temperature for 4 h under argon. Then the reaction

was quenched by adding excess ice-water and stirred for 30 min. The suspension was filtered and the residue was dried to afford 4-chloro-1-(4-chlorobenzyl)indoline-2,3-dione (1.34 g, 90%) as a red solid without further purification. This was directly used in the next step; $NH_2OH \cdot HCl$ (1.5 mmol) was added to a solution of 4-chloro-1-(4-chlorobenzyl)indoline-2,3-dione (1.4 mmol) in Pyridine (5 mL) and the resulting mixture was heated to 110 °C and stirred for 2 h. After cooling to room temperature, the resulting solution was poured into aqueous HCl (1 M, 50 mL) and extracted with EtOAc (3×50 mL). The combined organic layer was washed with brine (3×30 mL), dried over Na_2SO_4, concentrated under reduced pressure and then recrystallized to produce **5a** (382 mg, 85%) as a yellow solid. The derivatives **5b**, **5c** were prepared through this procedure by using 4-bromoindoline-2,3-dione and 4-iodoindoline-2,3-dione as material.

*4.2.1 4-chloro-1-(4-chlorobenzyl)-3-(hydroxyimino)indolin-2-one（**5a**）*

^{1}H NMR (400 MHz, DMSO-d_6): δ/ppm 13.73 (s, 1H, 3-NOH), 7.50 – 7.20 (m, 5H), 7.11 (d, J = 7.6 Hz, 1H), 6.95 (d, J = 7.6 Hz, 1H), 4.94 (s, 2H).^{13}C NMR (101 MHz, DMSO-d_6) δ/ppm 156.19-C2, 143.76, 141.90, 135.51, 132.59, 131.96, 129.62, 129.13, 127.69, 124.31, 116.54, 108.71, 42.26-*CH2*.

*4.2.2 4-bromo-1-(4-chlorobenzyl)-3-(hydroxyimino)indolin-2-one（**5b**）*

^{1}H NMR (400 MHz, DMSO-d_6): δ/ppm 13.75 (s, 1H, 3-NOH), 7.44 –

7.30 (m, 4H), 7.30 – 7.19 (m, 2H), 6.98 (dd, *J* = 7.6, 1.2 Hz, 1H), 4.93 (s, 2H).^{13}C NMR (101 MHz, DMSO-d_6) δ/ppm 156.25-C2, 143.94, 142.06, 135.46, 132.60, 132.05, 129.60, 129.13, 127.52, 118.24, 115.53, 109.12, 42.18-*CH2*.

4.2.3 1-(4-chlorobenzyl)-3-(hydroxyimino)-4-iodoindolin-2-one（***5c***）

^{1}H NMR (400 MHz, DMSO-d_6): δ/ppm 13.72 (s, 1H, 3-NOH), 7.58 – 7.48 (m, 1H), 7.39 (d, *J* = 8.8, 2H), 7.34 (d, *J* = 8.8 Hz, 2H), 7.05 (d, *J* = 8.0 Hz, 1H), 7.01 (d, *J* = 8.0 Hz, 1H), 4.92 (s, 2H); ^{13}C NMR (101 MHz, DMSO-d_6) δ/ppm 156.49-C2, 143.65, 141.98, 135.50, 134.20, 132.58, 131.89, 129.60, 129.11, 121.38, 109.57, 87.61, 41.96-*CH2*.

4.2.4

1-(4-chlorobenzyl)-3-(hydroxyimino)-4-(4-methoxyphenyl)indolin-2-one

*（**8a**）*

A mixture of 4-bromo-1-(4-chlorobenzyl)indoline-2,3-dione (**4b**) (351 mg, 1.0 mmol), (4-methoxyphenyl)boronic acid (167 mg, 1.1 mmol), $Pd(PPh_3)_4$ (116 mg, 0.1 mmol) and Cs_2CO_3 (6.52 mg, 2.0 mmol) in DMF (8 mL) was heated to 100 °C and stirred for 12 h under argon. After cooling to room temperature, the reaction mixture was poured into ice-water (60 mL) and extracted with DCM (3×30 mL). The combined organic layers were washed with brine (3×30 mL), dried over Na_2SO_4 and concentrated under reduced pressure. The crude product was purified by column chromatography on silica gel (petroleum ether/ethyl acetate 5:1)

to afford **7a** (272 mg, 72%) as a red solid. ^{1}H NMR (400 MHz, $CDCl_3$): δ/ppm 7.85 (s, 1H), 7.74 (d, *J* = 8.0, 1H), 7.66 – 7.42 (m, 6H), 7.07 – 7.02 (m, 2H), 6.91 (d, *J* = 8.0 Hz, 1H) 4.95 (s, 2H), 3.84 (s, 3H).

$NH_2OH·HCl$ (39 mg, 0.55 mmol) was added to a solution of **7a** (190 mg, 0.5 mmol) in Pyridine (3 mL) and the resulting mixture was heated to 110 °C and stirred for 2 h. After cooling to room temperature, the resulting solution was poured into aqueous HCl (1 M, 15 mL) and extracted with EtOAc (3×10 mL). The combined organic layer was washed with brine (3×15 mL), dried over Na_2SO_4, concentrated under reduced pressure and recrystallized to produce **8a** (149 mg, 76%) as a yellow solid. ^{1}H NMR (400 MHz, $CDCl_3$): δ/ppm 7.51 – 7.44 (m, 3H), 7.35 – 7.29 (m, 4H), 7.05 (d, *J* = 8.0, 1H), 6.98 (d, *J* = 8.8 Hz, 2H), 6.66 (d, *J* = 8.0 Hz, 1H), 4.93 (s, 2H), 3.88 (s, 3H); ^{13}C NMR (101 MHz, $CDCl_3$) δ/ppm 162.10-C2, 159.76-C3, 143.82, 141.77, 139.39, 134.17, 133.04, 131.02, 130.30, 130.27, 129.29, 128.78, 126.49, 115.12, 113.51, 108.37, 55.26-CH_3O, 42.76-CH_2; HRMS (ESI) m/z: Calcd for $C_{22}H_{17}ClN_2O_3Na$ $[M+Na]^+$ 415.0820; found, 415.0804.

4.2.5

1-(4-chlorobenzyl)-3-(hydroxyimino)-4-(4-(trifluoromethyl)phenyl)indolin-2-one （***8b***）

A mixture of **4b** (351 mg, 1.0 mmol), (4-*trifluoromethyl*phenyl)boronic acid (209 mg, 1.1 mmol), $Pd(PPh_3)_4$

(116 mg, 0.1 mmol) and Cs_2CO_3 (6.52 mg, 2.0 mmol) in DMF (8 mL) was heated to 100 °C and stirred for 12 h under argon. After cooling to room temperature, the reaction mixture was poured into ice-water (60 mL) and extracted with DCM (3×30 mL). The combined organic layers were washed with brine (3×30 mL), dried over Na_2SO_4 and concentrated under reduced pressure. The crude product was purified by column chromatography on silica gel (petroleum ether/ethyl acetate 5:1) to produce **7b** (312 mg, 75%) as a red solid. ^{1}H NMR (400 MHz, $CDCl_3$): δ/ppm 8.34 (d, *J* = 7.6, 1H), 7.86 (d, *J* = 7.6 Hz, 1H), 7.79 (d, *J* = 7.6 Hz, 1H), 7.72 (d, *J* = 8.0, 2H), 7.66 (d, *J* = 7.6 Hz, 2H), 7.62 (d, *J* = 8.0 Hz, 1H), 7.54 (t, *J* = 8.0, 1H), 7.06 (d, *J* = 7.6 Hz, 1H), 6.78 (d, *J* = 8.0 Hz, 1H), 4.95 (s, 2H).

7b (208 mg, 0.5 mmol) in Pyridine (3 mL) and the resulting mixture was heated to 110 °C and stirred for 2 h. After cooling to room temperature, the resulting solution was poured into aqueous HCl (1 M, 15 mL) and extracted with EtOAc (3×10 mL). The combined organic layer was washed with brine (3×15 mL), dried over Na_2SO_4, concentrated under reduced pressure and recrystallized to produce **8b** (153 mg, 71%) as a yellow solid. ^{1}H NMR (400 MHz, DMSO-d_6): δ/ppm 13.10 (s, 1H, 3-NOH), 7.78 (d, *J* = 8.4 Hz, 2H), 7.71 (d, *J* = 8.0 Hz, 2H), 7.44 – 7.39 (m, 5H), 7.03 (d, *J* = 8.0 Hz, 1H), 6.94 (d, *J* = 8.0 Hz, 1H), 4.98 (s, 2H); ^{13}C NMR (101 MHz, $CDCl_3$) δ/ppm 164.11-C2, 145.80, 144.44, 140.34,

133.88, 133.69, 132.22, 129.16, 128.77, 125.96, 124.04, 124.01, 113.37, 108.89, 43.27-*CH2*; HRMS (ESI) m/z: Calcd for $C_{22}H_{13}ClF_3N_2O_2$ $[M-H]^-$ 429.0623; found, 429.0602.

4.2.6 4-bromo-1-(4-chlorobenzyl)-3-(methoxyimino)indolin-2-one (***6b***)

K_2CO_3 (152 mg, 1.1 mmol) and CH_3I (156 mg, 1.1 mmol) were added to a stirred solution of **5b** (366 mg, 1.0 mmol) in dry DMF (5 mL). After the addition, the mixture was stirred at room temperature for 18 h. The reaction was poured into aqueous HCl (1 M, 50 mL) and extracted with EtOAc (3×20 mL). The organic layer was separated, washed with saturated NaCl (3×40 mL) and dried over anhydrous Na_2SO_4. After concentration to dryness under reduced pressure, the crude product was purified by column chromatography on silica gel (petroleum ether/ethyl acetate 10:1) to produce **6b** (258 mg, 68%) as a red solid. ^{1}H NMR (400 MHz, DMSO-d_6): δ/ppm 7.41 – 7.30 (m, 4H), 7.29 – 7.24 (m, 2H), 6.99 (dd, *J* = 1.2, 7.6 Hz, 1H), 4.93 (s, 2H), 4.21 (s, 3H); ^{13}C NMR (101 MHz, $CDCl_3$) δ/ppm 156.60, 143.71, 141.61, 133.84, 133.66, 131.33, 129.10, 128.81, 127.97, 117.96, 117.19, 107.96, 65.86, 42.86.

4.3. Biology evaluation

4.3.1 Materials and antibodies

All materials were from Sigma (St. Louis, MO, USA) unless otherwise stated. Commercial antibodies were purchased from the following sources: hTERT, anti-caspase-3 and β-actin (Santa Cruz

Biotechnology, Santa Cruz, CA, USA). Fluorophore and HRP-conjugated secondary antibodies were obtained from Invitrogen (Carlsbad, CA, USA).

4.3.2 Cell culture

Cell lines were obtained from the American Type Culture Collection, where they were characterized by DNA profiling. Cell lines were passaged for less than six months in this study. HeLa cells were grown at 37 °C and 5% CO_2 in Dulbecco's Modified Eagle Medium (DMEM) medium, supplemented with 10% fetal bovine serum (FBS).

4.3.3. Screening of potential inhibitors of hTERT expression

HeLa cells were plated at 2×10^6 cells/well in a 6-well plate. After 24 h, cells were transfected with 2 μg of P-3996 plasmid (hTERT promoter plasmid) [31] or 2 μg of pGL2 vector plasmid per well plus 0.1 μg of pCMV-β-galactosidase plasmid. After 24 h, the transfected cells were plated onto the 96-well plates at a density of 5×10^3cells/well. 24 h later, cells were treated with compounds at final concentrations of 5 μg/mL in DMEM containing 3% FBS (v/v) for 24 h. Luciferase activity was measured as described [32].

4.3.4 MTT assay

Cell proliferation was determined using the MTT (3-[4,5-dimethylthiazol-2-yl]-2,5- diphenyltetrazolium bromide; thiazolyl blue) assay. Cells were plated (5,000 cells/well) in triplicate with 200 μl

of growth medium in 96-well plates and cultured for the indicated period. Freshly prepared MTT was added at a final concentration of 0.5mg/ml in PBS pH 7.4 and plates incubated in the dark for 4 hours at 37 °C. The culture medium was then removed and the remaining blue precipitate was solubilized in dimethylsulfoxide (DMSO). The absorbance was read at 570nm in a microplate reader, and all the MTT data were averaged from 3 independent experiments each in triplicates. The IC_{50} value, defined as the drug concentration required to reduce cell survival to 50% determined by the relative absorbance of MTT, was assessed by probit regression analysis in SPSS statistical software [33].

4.3.5 Western blot

Cultured cells were washed twice in PBS before addition of ice cold lysis buffer (50 mM Tris–HCl pH 7.5, 150 mM NaCl, 1 mM NaF, 1 mM phenylmethylsulphonyl fluoride, 4 mg/ml leupeptin and 1 mg/ml aprotinin, and 1% Nonidet P-40). Equal amounts of protein were loaded into each well and separated by 7%, 10% or 12% SDS-PAGE gel, followed by transfer to nitrocellulose membrane. These were blocked in PBST buffer containing 5% non-fat dry milk for 1 hour at room temperature. Blots were then incubated overnight at 4 °C with primary antibodies. Secondary antibody incubation was carried out for 1 hour at room temperature. Finally, Odyssey infrared laser imaging system (LI-COR Biosciences, Lincoln, NE, USA) was used to image the

experimental results.

4.3.6 RNA extract and RT-PCR

Total RNA was isolated from cultured cells using Trizol reagent (Invitrogen, Carlsbad, CA, U.S.) according to the manufacturer's instructions. RNA was quantified by measuring the absorbance (A260 nm) and samples were then stored at –80°C until use. One microgram of total RNA was reverse transcribed with oligo (dT) primers using a reverse transcription system. The single-stranded cDNA was amplified by PCR using hTERT-specific primer and β-actin primer pairs. PCR was performed for 30 cycles (each cycle consisting of 94°C for 30 s, 54°C for 30 s, and 72°C for 30 s). The PCR products were analyzed by electrophoresis on a 1% agarose gel. Primer sequences used were as follows: hTERT-For CGGAAGAGTGTCTGGAGCAA, Rev GGATGAAGCGGAGTCTGGA; β-actin-For GGAATTCATGTCAGAACCGGCTGG, Rev CTCCTTAATGTCACGCACGATTTC.

4.3.7 Telomere length measurement

Telomere length was measured by a modified quantitative real time polymerase chain reaction (PCR)-based assay [22-23]. Briefly, the telomere repeat copy number to single gene copy number (T/S) ratio was determined using an Applied Biosystems StepOne™ thermocycler. The telomere reaction mixture consisted of 1× Qiagen Quantitect Sybr Green

Master Mix, 2.5mM of DTT, 270nM of Tel-1b primer (GGTTTTTGAGGGTGAGGGTGAGGGTGAGGGTGAGGGT), and 900nM of Tel-2b primer (TCCCGACTATCCCTATCCCTATCCCTATCCCTATCCCTA). The reaction proceeded for 1 cycle at 95°C for 5:00, followed by 40 cycles at 95°C for 15 seconds, and 54°C for 2 minutes. The 36B4 reaction consisted of 1×Bestar Sybr Green Master Mix, 300nM of 36B4U primer (CAGCAAGTGGGAAGGTGTAATCC), and 500nM of 36B4D primer (CCCATTCTATCATCAACGGGTACAA). The 36B4 reaction proceeded for 1 cycle at 95°C for 5 minutes, followed by 40 cycles at 95°C for 15 seconds, and 58°C for 1:10 minutes. All samples for both the telomere and single-copy gene reactions were performed in duplicate, and the threshold value for both reactions were set to 0.5. The relative telomere length was calculated as telomere repeat copy number to single-copy gene copy number (T/S ratio) in the study subjects as compared with that of a reference DNA sample. The relative T/S ratio estimated by real time PCR has been confirmed in previous work to be consistent with the Southern blot data [22].

4.3.8 DAPI staining assay

Cell apoptosis was evaluated by 4,6-diamidino-2-phenylindole (DAPI) staining. Cells were fixed in 5% paraformaldehyde, permeabilized with 0.1% Triton-X-100 in PBS, stained for 10 min with

DAPI (1 μg/mL), and analyzed by fluorescence microscopy. Cells were considered apoptotic when the nuclei showed chromatin condensation and fragmentation.

4.3.9 Apoptosis assay

Treated cells were collected and washed in PBS, and apoptosis was detected using an Annexin V-FITC Apoptosis Detection Kit (Cat. No KGA106 KeyGEN Bio-TECH, Nanjing, China) following the manufacturer's instructions. Cells were detected by flow cytometry and data were analyzed using CFlow 1.0.264.15 software.

4.3.10 Statistical analysis

All the experiments were repeated at least three times, the average values used as results and a set of representative figures shown as illustration. Statistical analysis was performed using the $\chi 2$ test or Fisher's exact test and Spearman's rank correlation coefficient analysis. $P<0.05$ indicated that the difference was significant, and $P<0.01$ indicated that the difference was highly significant.

Conflict of interest statement

All the authors have declared no conflict of interest.

Acknowledgements

We are grateful to Dr. Edward McKenzie (University of Manchester, UK) for critical reading of the manuscript. This research is supported by the National Natural Science Foundation of China grant (81402952).

Appendix A. Supplementary data

Supplementary data include MOL files and InChiKeys of the most important compounds described in this article.

Reference

[1] E.H. Blackburn, C.W. Greider, J.W. Szostak, Telomeres and telomerase: the path from maize, Tetrahymena and yeast to human cancer and aging, Nat Med, 12 (2006) 1133-1138.

[2] S.E. Holt, J.W. Shay, Role of telomerase in cellular proliferation and cancer, J Cell Physiol, 180 (1999) 10-18.

[3] T.M. Nakamura, G.B. Morin, K.B. Chapman, S.L. Weinrich, W.H. Andrews, J. Lingner, C.B. Harley, T.R. Cech, Telomerase catalytic subunit homologs from fission yeast and human, Science, 277 (1997) 955-959.

[4] Z.Y. Shen, L.Y. Xu, E.M. Li, W.J. Cai, M.H. Chen, J. Shen, Y. Zeng, Telomere and telomerase in the initial stage of immortalization of esophageal epithelial cell, World J Gastroenterol, 8 (2002) 357-362.

[5] M.P. Granger, W.E. Wright, J.W. Shay, Telomerase in cancer and aging, Crit Rev Oncol Hematol, 41 (2002) 29-40.

[6] J.W. Shay, S. Bacchetti, A survey of telomerase activity in human cancer, Eur J Cancer, 33 (1997) 787-791.

[7] N.W. Kim, Clinical implications of telomerase in cancer, Eur J Cancer, 33 (1997) 781-786.

[8] N.W. Kim, M.A. Piatyszek, K.R. Prowse, C.B. Harley, M.D. West, P.L. Ho, G.M. Coviello, W.E. Wright, S.L. Weinrich, J.W. Shay, Specific association of human telomerase activity with immortal cells and cancer, Science, 266 (1994) 2011-2015.

[9] L. Mansfield, A. Subramanian, H. Devalia, W. Jiang, R.F. Newbold, K. Mokbel, HTERT mRNA expression correlates with matrix metalloproteinase-1 and vascular endothelial growth factor expression in human breast cancer: a correlative study using RT-PCR, Anticancer Res, 27 (2007) 2265-2268.

[10] J. Lubin, J. Markowska, A. Markowska, J. Stanislawiak, T. Lukaszewski, Activity of telomerase in ovarian cancer cells. Clinical implications, Clin Exp Obstet Gynecol, 36 (2009) 91-96.

[11] M.N. Helder, S. Jong, E.G. Vries, A.G. Zee, Telomerase targeting in cancer treatment: new developments, Drug Resist Updat, 2 (1999) 104-115.

[12] K. Sekhri, Telomeres and telomerase: understanding basic structure and potential new therapeutic strategies targeting it in the treatment of cancer, J Postgrad Med, 60 (2014) 303-308.

[13] S.A. Stewart, R.A. Weinberg, Telomerase and human tumorigenesis, Semin Cancer Biol, 10 (2000) 399-406.

[14] K.M. Burchett, Y. Yan, M.M. Ouellette, Telomerase inhibitor Imetelstat (GRN163L) limits the lifespan of human pancreatic cancer cells, PLoS One, 9 (2014) e85155.

[15] Z.G. Dikmen, G.C. Gellert, S. Jackson, S. Gryaznov, R. Tressler, P. Dogan, W.E. Wright, J.W. Shay, In vivo inhibition of lung cancer by GRN163L: a novel human telomerase inhibitor, Cancer Res, 65 (2005) 7866-7873.

[16] P.A. Waghorn, M.R. Jackson, V. Gouverneur, K.A. Vallis, Targeting telomerase with radiolabeled inhibitors, Eur J Med Chem, 125 (2017) 117-129.

[17] Q.P. Qin, J.L. Qin, T. Meng, W.H. Lin, C.H. Zhang, Z.Z. Wei, J.N. Chen, Y.C. Liu, H. Liang, Z.F. Chen, High in vivo antitumor activity of cobalt oxoisoaporphine complexes by targeting G-quadruplex DNA, telomerase and disrupting mitochondrial functions, Eur J Med Chem, 124 (2016) 380-392.

[18] J.B. Shi, L.Z. Chen, Y. Wang, C. Xiou, W.J. Tang, H.P. Zhou, X.H. Liu, Q.Z. Yao, Benzophenone-nucleoside derivatives as telomerase inhibitors: Design, synthesis and anticancer evaluation in vitro and in vivo, Eur J Med Chem, 124 (2016) 729-739.

[19] Y.Y. Chen, X.Q. Wu, W.J. Tang, J.B. Shi, J. Li, X.H. Liu, Novel dihydropyrazole-chromen: Design and modulates hTERT inhibition proliferation of MGC-803, Eur J Med Chem, 110 (2016) 65-75.

[20] K.L. Han, Y.S. Li, Y.Z. Zhang, Y.O. Teng, Y. Ma, M.Y. Wang, R.L. Wang, W.R. Xu, Q.W. Yao, Y.M. Zhang, H.J. Qin, H. Sun, P. Yu, Design, synthesis and docking study of novel tetracyclic oxindole derivatives as alpha-glucosidase inhibitors, Bioorganic & Medicinal Chemistry Letters, 25 (2015) 1471-1475.

[21] H. Sun, Y. Li, X. Zhang, Y. Lei, W. Ding, X. Zhao, H. Wang, X. Song, Q. Yao, Y. Zhang, Y. Ma, R. Wang, T. Zhu, P. Yu, Synthesis, alpha-glucosidase inhibitory and molecular docking studies of prenylated and geranylated flavones, isoflavones and chalcones, Bioorg Med Chem Lett, 25 (2015) 4567-4571.

[22] R.M. Cawthon, Telomere measurement by quantitative PCR, Nucleic Acids Research, 30 (2002).

[23] H. Wang, H.L. Chen, X. Gao, M. McGrath, D. Deer, I. De Vivo, M.A. Schwarzschild, A. Ascherio, Telomere length and risk of Parkinson's disease, Movement Disord, 23 (2008) 302-305.

[24] R.M. Siegel, Caspases at the crossroads of immune-cell life and death, Nat Rev Immunol, 6 (2006) 308-317.

[25] M.G. Grutter, Caspases: key players in programmed cell death, Curr Opin Struct Biol, 10 (2000) 649-655.

[26] W.C. Earnshaw, L.M. Martins, S.H. Kaufmann, Mammalian caspases: structure, activation, substrates, and functions during apoptosis, Annu Rev Biochem, 68 (1999) 383-424.

[27] O. Julien, J.A. Wells, Caspases and their substrates, Cell Death Differ, 24 (2017) 1380-1389.

[28] E. Miri-Moghaddam, A. Deezagi, Z.S. Soheili, P. Shariati, Apoptosis and reduced cell proliferation of HL-60 cell line caused by human telomerase reverse transcriptase inhibition by siRNA, Acta Haematol, 124 (2010) 72-78.

[29] C. Park, G.Y. Kim, W.I. Kim, S.H. Hong, D.I. Park, N.D. Kim, S.J. Bae, J.H. Jung, Y.H. Choi, Induction of apoptosis by (Z)-stellettic acid C, an acetylenic acid from the sponge Stelletta sp., is associated with inhibition of telomerase activity in human leukemic U937 cells, Chemotherapy, 53 (2007) 160-168.

[30] Y.Q. Zhong, Z.S. Xia, Y.R. Fu, Z.H. Zhu, Knockdown of hTERT by SiRNA suppresses growth of Capan-2 human pancreatic cancer cell via the inhibition of expressions of Bcl-2 and COX-2, J Dig Dis, 11 (2010) 176-184.

[31] Y.S. Cong, J. Wen, S. Bacchetti, The human telomerase catalytic subunit hTERT: organization of the gene and characterization of the promoter, Hum Mol Genet, 8 (1999) 137-142.

[32] Y. Li, A. Guo, Y. Feng, Y. Zhang, J. Wang, L. Jing, Y. Yan, Z. Liu, L. Ma, A. Diao, Sp1 transcription factor promotes TMEPAI gene expression and contributes to cell proliferation, Cell Prolif, (2016).

[33] Y. Li, L. Zhang, J. Zhou, S. Luo, R. Huang, C. Zhao, A. Diao, Nedd4 E3 ubiquitin ligase promotes cell proliferation and autophagy, Cell Prolif, 48 (2015) 338-347.

Figure legend

Scheme 1 Synthesis of isatin derivatives (5a-5c, 6b). Reagents and conditions: (a) Na2SO4, NH2OH HCl, CCl3CH(OH)2, 2M HCl, H2O, 90℃, 2 h; (b) conc. H2SO4, 65℃, 30 min; (c) K2CO3, DMF, 60℃, 2 h; (d) Pyridine, NH2OH HCl, 110℃, 2h; (e) CH3I, K2CO3, DMF, 25℃, 12h

Scheme 2 Synthesis of isatin derivatives (**8a-8b**). Reagents and conditions: (a) Pd(PPh3)4, Cs2CO3, DMF, 100 ℃; (b) Pyridine, NH2OH HCl,110℃, 2h.

Figure 1 Compound 5c inhibits hTERT gene promoter activity. (A) HeLa cells were transfected with P-3996 plasmid or pGL2 vector per well plus pCMV-β-galactosidase plasmid, then treated with the compounds (5μM). Cells were treated with 0.1% (v/v) DMSO to act as the negative control. Results are expressed as the fold activity over the activity of the negative control. The screening assay was repeated three times and partial data are shown. (B) HeLa cells were co-transfected with promoter-3996 or pGL2 vector and pCMV-β-galactosidase plasmid. 24 h after compound 5c (1, 2, 4, 8 and 16μM) treatment, luciferase activity was measured and normalized using β-galactosidase activity. Results are expressed as the fold activity over the activity of the negative control.

Figure 2 Compound **8b** inhibits hTERT expression in cancer cells (A) HeLa cells were treated with 5μM of compound **8b** for 24h and then hTERT mRNA levels were analyzed using RT-PCR, β-actin was used as an internal control to check the efficiency of cDNA synthesis and PCR amplification. (B) Quantification of RT-PCR for hTERT mRNA levels using ImageJ software. (C) HeLa cells were treated with compound **8b** (1, 2, 4, 8 and 16μM) for 24 h, and 0.1% (v/v) DMSO was used as a negative control. Cells were then lysed and hTERT expression was analyzed by Western blot. (D) Quantification of Western blot for hTERT levels using ImageJ software. (E) HeLa cells were treated with 5μM of compound **8b** for 12, 24, 36 and 48h and then cells were lysed and hTERT expression was analyzed by Western blot. (F) Quantification of Western blot for hTERT levels using ImageJ software. (G) HeLa cells were treated with compound **8b** or DMSO for 22 generations, and measured the relative length of telomeres using Q-PCR (**P < 0.01 VS Control).

Figure 3 Knockdown of endogenous hTERT in HeLa cells by RNA interference inhibits cell proliferation (A) HeLa cells were infected with 200 μl lentiviruses expressing shhTERT-1#, shhTERT-2# or the scrambled control, and expression of hTERT was detected by Western blot. (B) HeLa cells were infected with 200 μl lentiviruses expressing

shhTERT-1#, shhTERT-2# or the scrambled control, and t cell proliferation was analyzed by MTT assay at 1d, 2d and 3d post-infection. (C) HeLa expressing shhTERT-1#, shhTERT-2# or the scrambled control were used for colony formation assays after 3 weeks culture, then the plates were photographed. (D) Quantification of the efficiency of colony formation by statistical analysis.

Figure 4 Compound **8b** inhibits HeLa cell proliferation (A) The HeLa and L02 cells were treated with an increasing gradient concentration of compound **8b** (1, 2, 4, 8 and 16 μM) for 48 h followed by MTT analysis . (B) HeLa cells were treated with 5 μM compound **8b** for 24 or 48 h followed by the MTT assay. (C) HeLa cells treated with 5 μM compound **8b** were used for colony formation assay. The plates were photographed after 3 weeks culture. (D) Quantification of the efficiency of colony formation by statistical analysis.

Figure 5 Compound **8b** induced cell apoptosis via a mitochondrial-dependent pathway (A) HeLa cells were treated with compound **8b** for 48h, and then stained with DAPI. The arrows highlight cells undergoing apoptosis. (B) HeLa cells were treated with compound **8b** for 48h, then double-labeled with Annexin V/PI staining. Cells were detected by flow cytometry and data were analyzed using CFlow 1.0.264.15 software. (C)

HeLa cells were treated with compound **8b** for 24h, and analyzed by Western blot using antibodies against cleaved caspases 3, cleaved caspases 9, Bax, Bcl-2 and β-actin.

Table 1 The effect of 6 compound **5c** analogs on *hTERT* gene promoter activity

Chemical number	Chemical name	Chemical structure	EC_{50} (μM)
5a	*4-chloro-1-(4-chlorobenzyl)-3-(hydroxyimino)indolin-2-one*	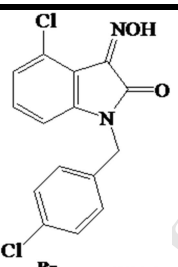	13
5b	*4-bromo-1-(4-chlorobenzyl)-3-(hydroxyimino)indolin-2-one*	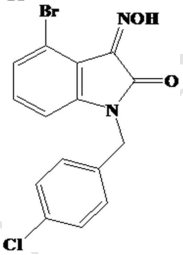	6
5c	*1-(4-chlorobenzyl)-3-(hydroxyimino)-4-iodoindolin-2-one*	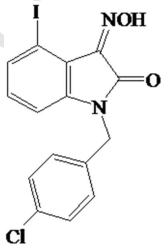	14
6b	*4-bromo-1-(4-chlorobenzyl)-3-(methoxyimino)indolin-2-one*	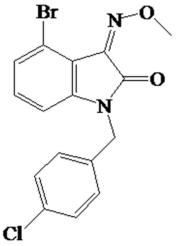	None
8a	*1-(4-chlorobenzyl)-3-(hydroxyimino)-4-(4-methoxyphenyl)indolin-2-one*	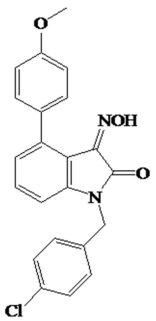	12
8b	*1-(4-chlorobenzyl)-3-(hydroxyimino)-4-(4-(trifluoromethyl)phenyl)indolin-2-one*	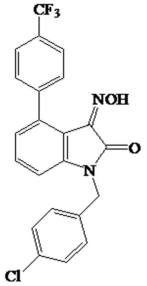	5

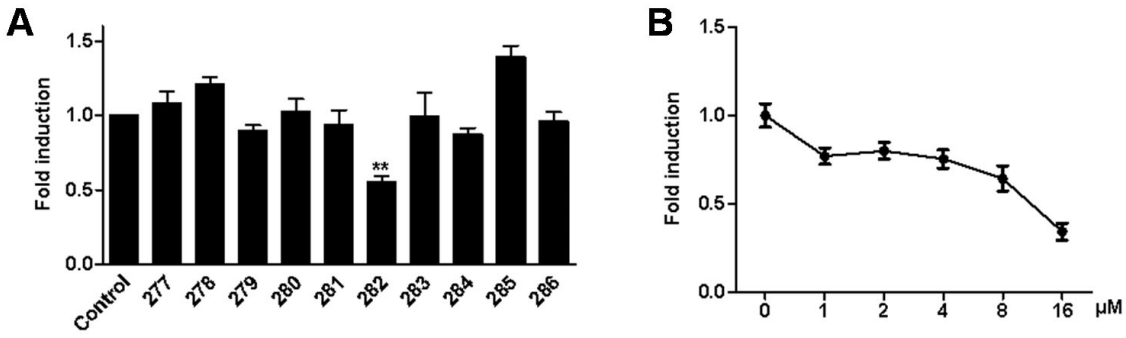

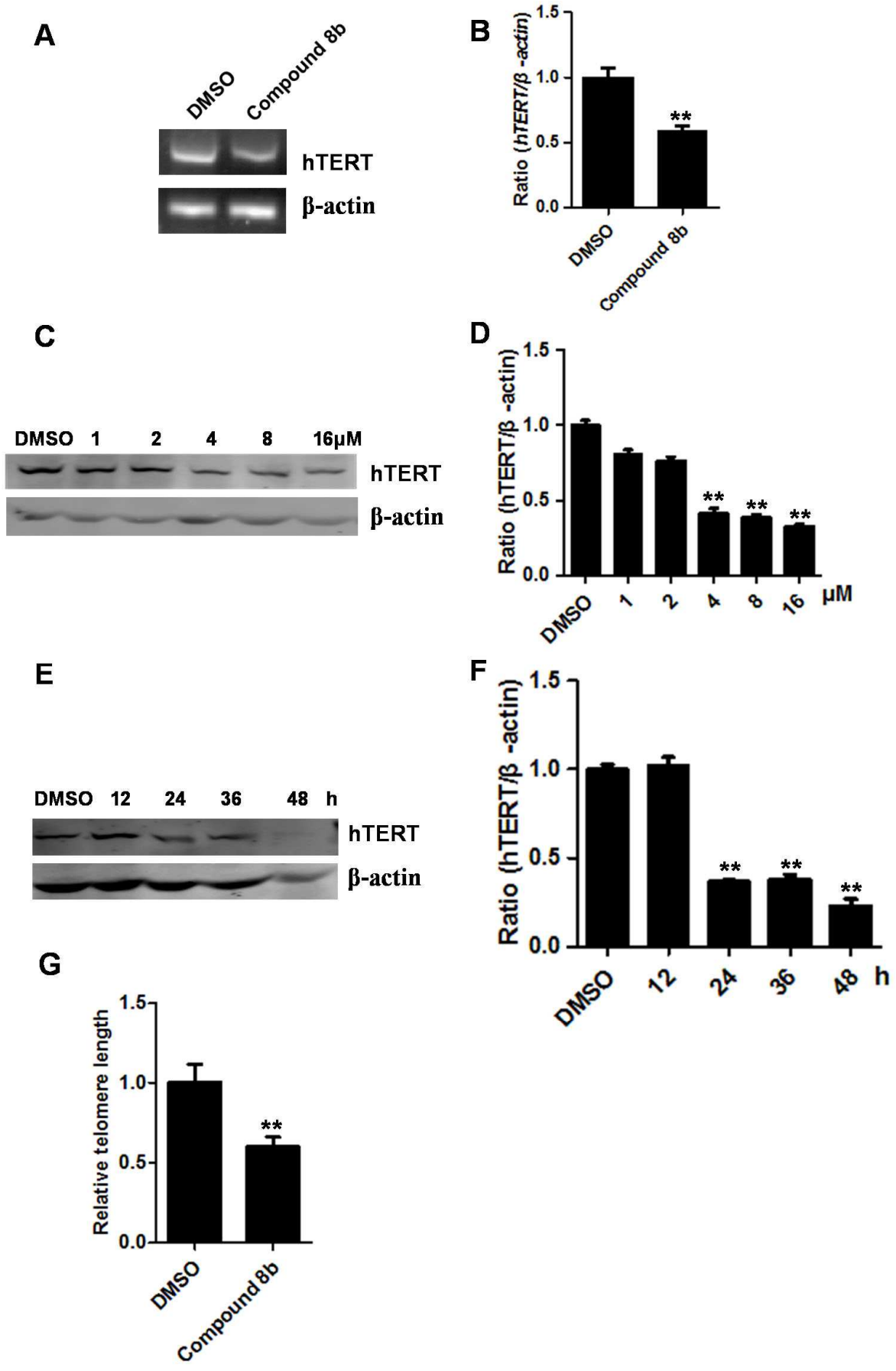
A
DMSO
Compound 8b
hTERT
β-actin
B
Ratio (hTERT/β -actin)
1.5
1.0
0.5
0.0
**
DMSO
Compound 8b
C
DMSO 1 2 4 8 16μM
hTERT
β-actin
D
Ratio (hTERT/β -actin)
1.5
1.0
0.5
0.0
**
**
**
DMSO 1 2 4 8 16 μM
E
DMSO 12 24 36 48 h
hTERT
β-actin
F
Ratio (hTERT/β -actin)
1.5
1.0
0.5
0.0
**
**
**
DMSO 12 24 36 48 h
G
Relative telomere length
1.5
1.0
0.5
0.0
**
DMSO
Compound 8b

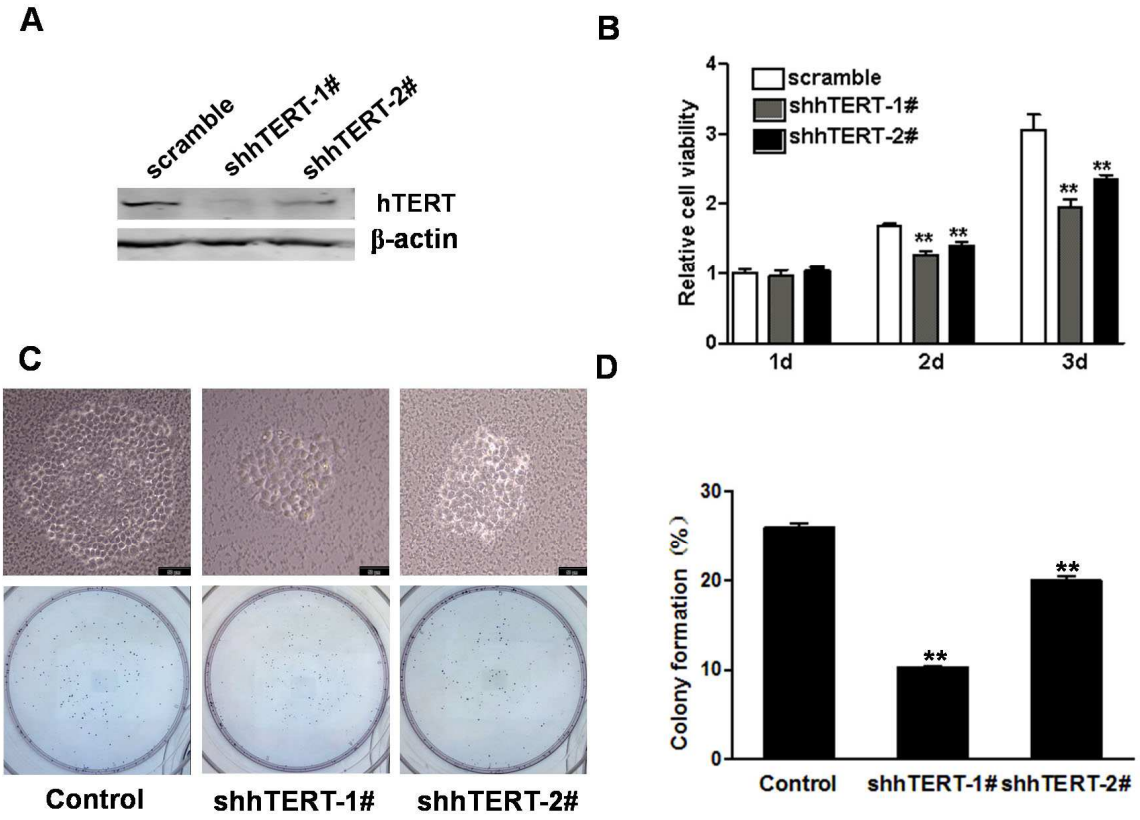

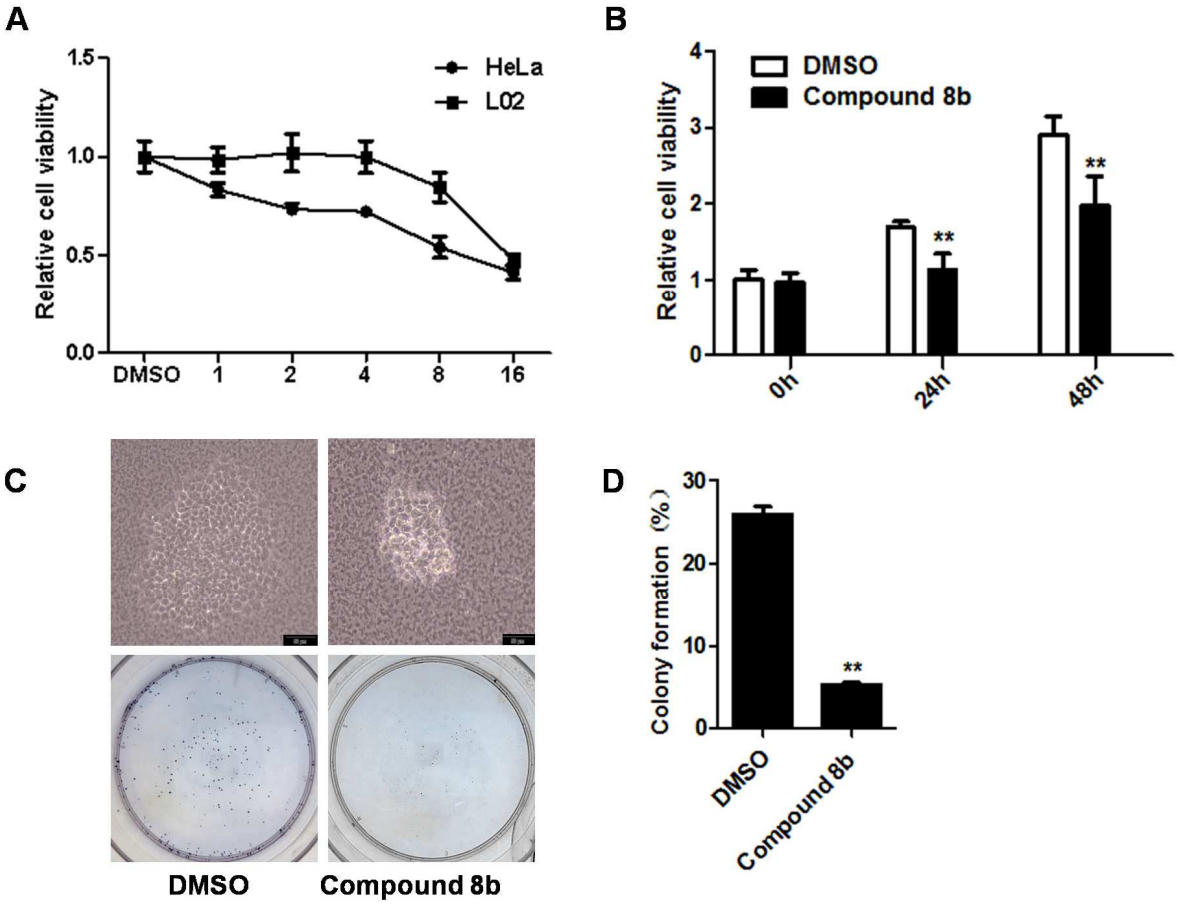

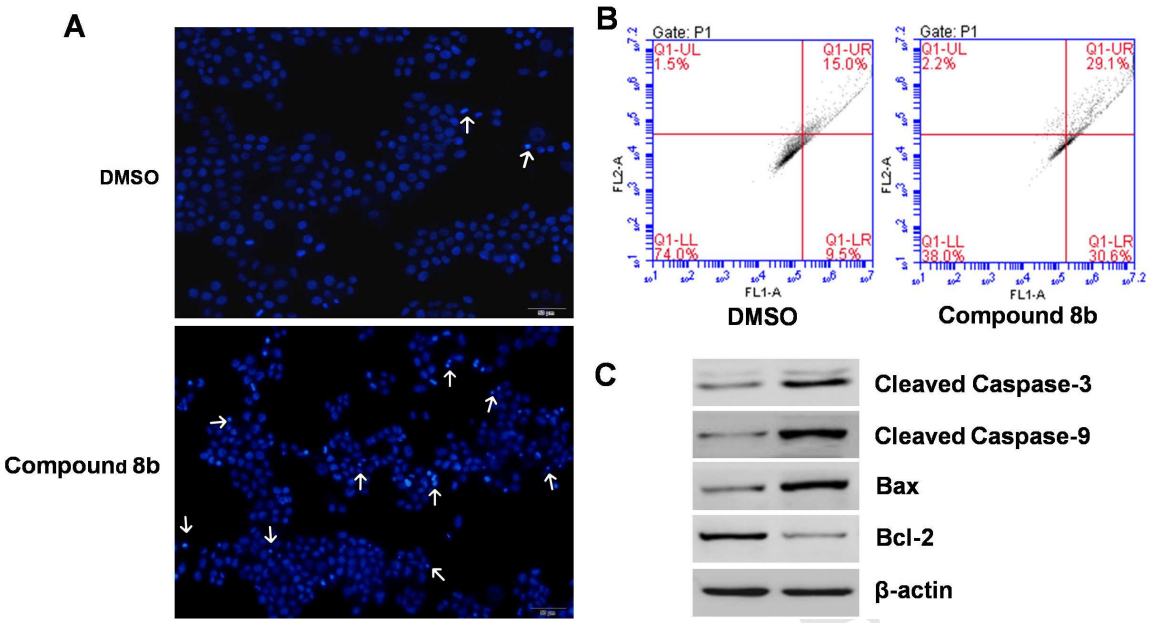

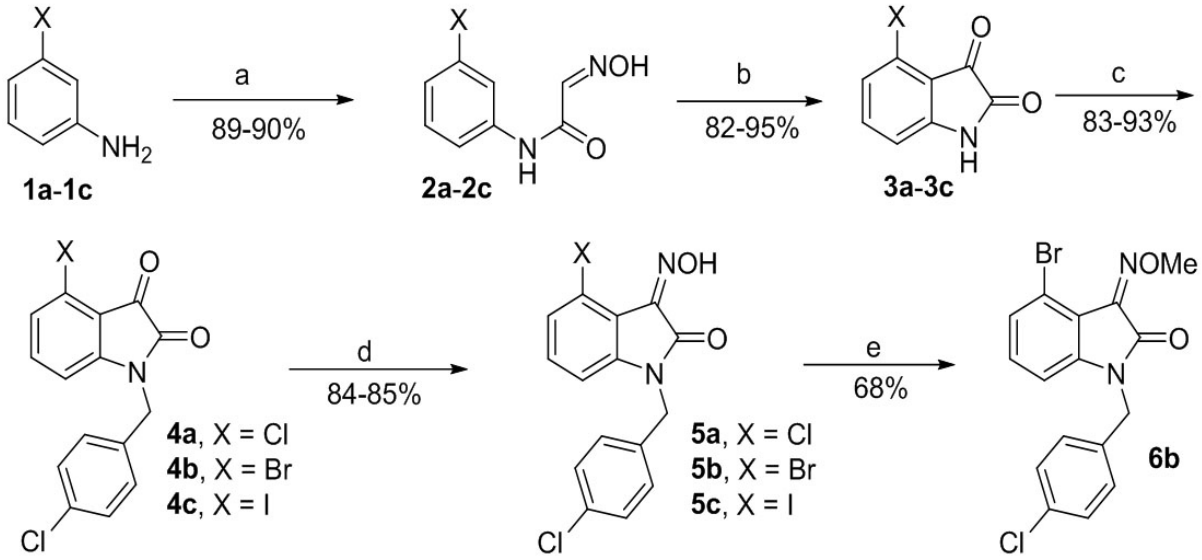

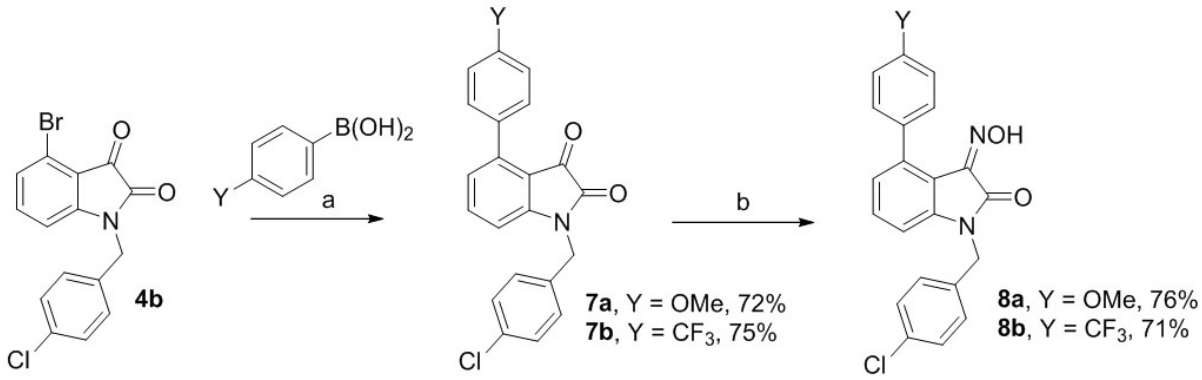

Highlights:

- Compound **8b** inhibits hTERT expression in cancer cells.
- Compound **8b** inhibits HeLa cell proliferation.
- Compound **8b** induced cell apoptosis via mitochondrial-dependent pathway.